JOURNAL OF AGRICULTURAL AND FOOD CHEMISTRY

Analysis of Protein Structures and Interactions in Complex Food by Near-Infrared Spectroscopy. 1. Gluten Powder

SUSANNE WRANG BRUUN, IB SØNDERGAARD, AND SUSANNE JACOBSEN*

Enzyme and Protein Chemistry, BioCentrum-DTU, Søltofts Plads, Building 224, Technical University of Denmark, DK-2800 Kgs. Lyngby, Denmark

The potential of near-infrared (NIR) spectroscopy in detailed food analysis was tested in a model system consisting of gluten powder treated with moisture and heat. Second-derivative transformation and extended multiplicative signal correction were applied for improving the band resolution and removing physical and quantitative spectral variations. Subsequent chemometric analyses gave loading spectra, which were interpreted as spectral effects of altered protein structures, induced by the treatments. Moistening of the gluten powder resulted in shifts and intensity changes in the protein bands, which could be explained by a combination of minor secondary structure changes, water binding, and changed microenvironments of the amino acid side chains. Heat denaturation induced increases at 2209 nm and decreases at 2167−2182 nm, indicating an α-helix to β-sheet transformation, in agreement with the expectations.

KEYWORDS: Chemometrics; extended multiplicative scatter correction (EMSC); near-infrared spectroscopy (NIR); gluten; heat treatment; hydration; protein secondary structure; principal component analysis (PCA); partial least-squares (PLS) regression; spectral pretreatment

INTRODUCTION

Food properties, such as texture, taste, and mouthfeel, are highly dependent on structures and interactions of the constituting macromolecules, because they govern the physicochemical properties of, for example, proteins and polysaccharides (*1*). However, only a few methods, such as nuclear magnetic resonance (NMR) and Raman and Fourier transform infrared (FTIR) spectroscopy, are useful for analyzing the intact food samples for providing this type of information. These methods may be applied in the food industry for quality control and in some cases even for in-line/on-line process monitoring (*2*).

In this study we investigate the ability of near-infrared (NIR) spectroscopy to detect protein structure and interaction changes in a complex food system (gluten) and thereby to give detailed information on the food quality and on structure−functionality relations. Although NIR spectroscopy is most often used for quantitative chemical analyses and seldom for structure determination, its use in detailed food studies could have several advantages. Essentially, NIR spectroscopy can measure many types of samples without sample preparation, and, together with the short sampling times, this makes NIR more suited for on-line applications than the related FTIR method.

FTIR spectroscopy, involving absorptions in the mid-infrared (MIR) region of the electromagnetic spectrum due to vibrational excitations, has long been used for the determination of protein secondary structures of proteins in the solid state, in membranes, and in solutions (*3*). The studies have most often involved analysis of the amide I band (1700−1600 cm^{-1}), reflecting mainly C═O stretching vibrations in the peptide groups. In the broad amide I envelope, the different secondary structures absorb at specific frequency intervals as a result of a sensitivity of the amide I mode toward hydrogen-bonding strength and couplings between the peptide groups (e.g., transition dipole couplings) (*4*). Also, the amide II band (N−H deformation coupled with C−N stretching) and the amide III band (N−H deformation coupled with CH_2 deformation) are sensitive to the protein structures, although the relationships are less clear (*4*).

FTIR studies have provided important information on the gluten protein structures (*5*). An interest in gluten protein structures and the physicochemical basis of gluten viscoelasticity has emerged in the past decade, and several models of the gluten network have been suggested, for example, with the purpose of explaining its viscoelastic behavior (*6*, *7*). This topic has interest not only in relation to the baking process but also for the processing of gluten into biodegradable films.

The gluten proteins are broadly divided into the monomeric gliadins and the polymeric glutenins, of which the glutenins are able to form intermolecular S−S bridges and thereby very large and insoluble polymers (*8*). Although the S−S bridges play a major role in gluten functionality, non-covalent interactions are important as well (*8*). Both glutenin and gliadin are rich in proline and glutamine, which appear in the repetitive domains of the proteins. These domains consist of short repeat sequences and have been found to adopt the structure of a loose β-spiral in solution (*8*, *9*). However, by use of attenuated total

* Corresponding author (telephone +45 45252741; fax +45 4588 6307; e-mail sja@biocentrum.dtu.dk).

10.1021/jf063680j CCC: $37.00
Published on Web 08/03/2007

reflectance (ATR)-FTIR, Pezolet et al. (*9*) were the first to demonstrate that gluten proteins in the solid hydrated state form intermolecular β-sheets not seen in solution. The detection of this structure has led to development of the "loop and train" model for glutenin, which can explain the viscoelastic properties of gluten (*6*, *10*). A limitation of ATR-FTIR is that these spectra contain information about only the sample surfaces, and for gluten, this may give rise to mistaken conclusions, because the protein structures and interactions are very sensitive to the sample histories (e.g., previous sample handling and cutting) and degree of hydration (*10*, *11*).

The overtone and combination bands in the more energy-rich NIR region at 750−2500 nm show lower absorptivities than MIR bands, and NIR spectroscopy is able to characterize also the deeper layers of the samples. Thus, NIR spectroscopy is less prone to errors from sample inhomogeneities. (Still, NIR light penetrates only a few millimeters into the samples.) Further advantages of NIR spectroscopy compared to ATR-FTIR are the higher speed of the measurements and no need for an expensive ATR crystal. One drawback of NIR spectroscopy is that the multiple overtone and combination bands in the spectra of biological samples greatly overlap each other and cause broad and unresolved bands, which cannot be assigned to single chemical groups. Therefore, the common way to extract information from NIR spectra is to apply chemometric methods such as principal component analysis (PCA) and partial least-squares (PLS) regression for making classification or calibration models, without the need for interpreting the spectra.

In this work, we consider the ability of NIR spectroscopy to detect changes in gluten protein structures and interactions when the gluten powder is modified by increasing water content and heat treatment. A spectral interpretation is done by comparison to existing knowledge of gluten proteins obtained in ATR-FTIR and NMR studies.

MATERIALS AND METHODS

Gluten Preparation. Two different gluten fractions (glutens A and B) were prepared by wash out from a dough according to the following procedure: 100 g of commercial wheat flour (Amo, Denmark) was mixed with 50 mL of distilled water and kneaded for 2 min. Gluten was washed out by five washings in 1 L of distilled water (gluten A) or in 1 L of 2% NaCl solution (gluten B). The last wash was carried out in distilled water for each preparation. The gluten fraction was freeze-dried and milled in an IKA A10 laboratory mill (IKA Labortechnik, Staufen, Germany); 3 g aliquots were milled for 15−20 s, and the powder was sifted through a sieve with a mesh size of 500 μm. The gluten powder was kept at room temperature above drying agent in a sealed container for further use. This procedure results in a gluten fraction with ∼80% protein.

A starch fraction was isolated from a dough as well.

The initial moisture contents (mc) of the freeze-dried gluten preparations were determined by oven-drying: 1 g of each gluten fraction was heated in the oven at 120 °C until a constant weight was obtained, and the mc was calculated from the initial and final sample weights. The preparations contained 3.3−4.3% mc.

Gluten at Different Moisture Contents. *Time Series Hydration.* Six aliquots of ∼700 mg of gluten A were spread on Petri dishes, inserted into a sealed container with water in the bottom, and kept either at room temperature or at 5 °C. After storage for different time intervals (t = 1, 2, 3, 4, 23, 27, 45, and 53 h), each sample was weighed to obtain the water content, and a NIR spectrum was immediately obtained before the sample was returned to the container. After storage for 4 h, two of the samples were transferred to a sealed container with drying agent. All of the above gluten treatments were carried out in two replicates.

Starch was moistened in a similar way for 20, 24, 42, and 50 h before the NIR spectra were obtained.

Hydration in Humidity Chambers. Other gluten samples were moistened for an equal time period in humidity chambers of different relative humidities (RHs). For both glutens A and B, one aliquot (∼700 mg) was placed above a saturated $MgCl_2$ solution (∼33% RH), another aliquot was placed above a saturated NaCl solution (∼75.5% RH), and two others were placed above distilled water, all in sealed containers kept at room temperature. One sample above distilled water was returned to a drying chamber after moistening for 24 h. After 40 h of storage, the samples were weighed, and the NIR spectra were obtained (with two measurement replicates). Totally, the hydration experiment includes 78 spectra.

The mc was calculated on a wet basis from the sample weights obtained before and after moistening. The purpose of this study was not to evaluate the performance of NIR spectroscopy for water content determination in gluten and, therefore, the accuracy of the reference values is not important.

Heat Treatment. Commercial gluten powder (Sigma-Aldrich catalog no. G5004) was moistened in a humid chamber at 5 °C for 65 h to a water content of 20−25%. Then, aliquots of ∼700 mg were filled in Eppendorf tubes and heated in a water bath. The heat treatments involved heating at 65 °C for 0.5 h or at 85 °C for 0.5, 1, or 1.5 h. As control, a dry gluten powder sample was heated at 85 °C for 0.5 h (no denaturation is expected). In addition, a moistened gluten sample was not heated but placed above a drying agent in a closed chamber at room temperature for 4 h to determine the effect of drying. All samples were cooled to room temperature, ground to powder, and measured immediately by NIR spectroscopy with two to four measurement replicates. The denaturation experiment includes 56 spectra.

NIR Analysis. The gluten and starch spectra were obtained in reflectance mode from 790 to 2500 nm on a Perkin-Elmer, Spectrum One, FT-NIR instrument, equipped with a reflectance assessory and an InGaAs detector. The nominal resolution was 8 cm^{-1}, and 50 scans were co-added. The data interval was 1.67 nm. The samples were measured in a sample cup, and the powder was slightly compressed with a spatula before the measurement.

Spectral Pretreatment. The pretreatments included second-derivative transformation (Savitzky−Golay derivation, with seven data point smoothing) and extended multiplicative signal correction (EMSC) (*12*). The two preprocessing methods were used in combination as described under Results and Discussion.

The EMSC model (*12*) is based on an approximation of the absorbance spectrum $\mathbf{z}_i$ as a "physically" modified version of the chemically based spectrum $\mathbf{z}_{i,\mathrm{chem}}$. One purpose of EMSC is to remove these modifications, which are represented by both an additive polynomial baseline effect and a multiplicative scaling effect:

$$\mathbf{z}_i \approx b_i \cdot \mathbf{z}_{\mathrm{chem},i} + a_i \cdot \mathbf{1} + d_i \cdot \tilde{\nu} + e_i \cdot \tilde{\nu}^2 \quad (1)$$

Here, the coefficient b_i represents the multiplicative scaling effect, the coefficients a_i, d_i, and e_i represent the additive baseline deviations, and $\tilde{\nu}$ is the linear wavelength range ν between −1 and +1. Another purpose of EMSC is to remove spectral interferences of chemical origin. The "chemical" spectrum for sample i is approximated by

$$\mathbf{z}_{\mathrm{chem},i} = \mathbf{m} + \sum_{a=1}^{A_{\mathrm{bad}}+A_{\mathrm{good}}} t_{i,a}\mathbf{p}_a = \mathbf{m} + \mathbf{t}_i\mathbf{P} \quad (2)$$

In eq 2, $\mathbf{m}$ is the mean spectrum or another reference spectrum, $\mathbf{P}$ contains the loading spectra ($\mathbf{p}_a$) of the known chemical constituents, and $\mathbf{t}_i$ holds their concentrations in sample i. The first A_{bad} loading spectra represent the "bad" spectral components, for example, from unwanted constituents, and they will be modeled and subtracted. The last A_{good} loading spectra represent the components of interest, and they will be kept but are included for avoiding alias problems in the "bad" components. After combination of eqs 1 and 2, least-squares estimation yields the model coefficients, and the corrections are performed according to

$$\mathbf{z}_{i,\mathrm{corrected}} = (\mathbf{z}_i - \sum_{a=1}^{A_{\mathrm{good}}+A_{\mathrm{bad}}} \hat{h}_{i,a}\delta_a\mathbf{p}'_a - \hat{a}_i 1 - \hat{d}_i\tilde{\nu} - \hat{e}_i\tilde{\nu})/\hat{b}_i \quad (3)$$

where $\hat{\mathbf{t}}_i = \hat{\mathbf{h}}_i/\hat{b}_i$, and $\delta_a = 1$ for "bad" components and $\delta_a = 0$ for "good" components.

We term the preprocessing a "physical" EMSC when $\mathbf{z}_{i,\text{chem}}$ is simply approximated by the mean spectrum **m**, whereas we term it a "physical−chemical" EMSC when chemical model spectra are included in the description. EMSC modeling is further described in Martens et al. (*12*). All pretreatments were carried out in Unscrambler version 9.2 (Camo, Oslo, Norway).

Data Analysis. PCA and PLS regressions with cross-validation were carried out in Unscrambler version 9.2. For the resulting score and loading vectors, the designations $\mathbf{t}_a$ and $\mathbf{p}_a$, respectively, are used again, and approximation of the spectrum for sample i ($\mathbf{x}_i$) is done according to eq 4

$$\mathbf{x}_i = \mathbf{m} + t_{1,i}\cdot\mathbf{p}_1 + t_{2,i}\cdot\mathbf{p}_2 + ... + t_{A,i}\cdot\mathbf{p}_A \quad (4)$$

where **m** is the mean spectrum and A is the selected number of PCs.

Marten's uncertainty test, based on cross-validation and jack-knifing, was carried out for reliability and significance testing of the variables in the PLS models, and variables with nonsignificant regression coefficients were removed for improving the models. The test is based on the re-estimation of the model parameters in each of the subsamplings during cross-validation, because the pertubations of the parameter estimates compared to the full model parameters give measures of the parameter uncertainty/stability.

RESULTS AND DISCUSSION

Gluten Hydration. Water acts as a plasticizer in the dry gluten proteins, decreasing their glass transition temperature T_g below room temperature and transforming the brittle and dry material into a soft and deformable substance. The transition from glassy to rubbery state during hydration is caused by the increased gluten−water interaction and is associated with increased protein side-chain and backbone mobility (*13*) and unfolding of the tightly packed and aggregated proteins, thus allowing the proteins to establish the proper interactions for development of the viscoelastic gluten network. In the "loop and train model" of the gluten network (*6*, *10*), glutenin is explained as existing as either hydrated chains, that is, the "loops" or as "trains", in which intermolecular β-sheets and hydrophobic interactions establish contacts between two or more chains. At a point in the hydration, further increase of water content leads to an increase of the mobile loop regions, consisting of hydrated extended structures and β-turns at the expense of the train regions (*14*).

Water Uptake. The moisture contents obtained for gluten powder samples by hydration over time and by hydration in chambers of different humidities are shown in panels **a** and **b** of **Figure 1**, respectively. **Figure 1a** shows that samples stored at 25 °C (G25 samples) took up water more easily than the samples stored at 5 °C (G05 samples) and obtained somewhat higher water contents. Increased water absorption for gluten stored above its T_g has been explained by an increased exposure of polar groups, which can interact with water (*15*). The glass transition for gluten at 25 °C has been found to take place above ∼10% mc (*13*), and the somewhat higher water absorptions observed for the G25 samples at 10% mc and higher may thus be accounted for by this phenomenon. The rubbery state of these samples was supported by their soft texture. Likewise, the increased water absorption for gluten B compared to gluten A (**Figure 1b**) could stem from increased exposure of polar and ionic groups upon salt treatment of gluten B (gluten B was washed out with a 2% NaCl solution, whereas gluten A was washed out with distilled water). As the salt treatment may also have led to greater washout of lipids from gluten B, a higher protein content could also explain the increased water absorption. Furthermore, different protein compositions of the gluten fractions could be an additional explanation of the different water uptakes, because the albumins and globulins have increased solubilities in salt solution.

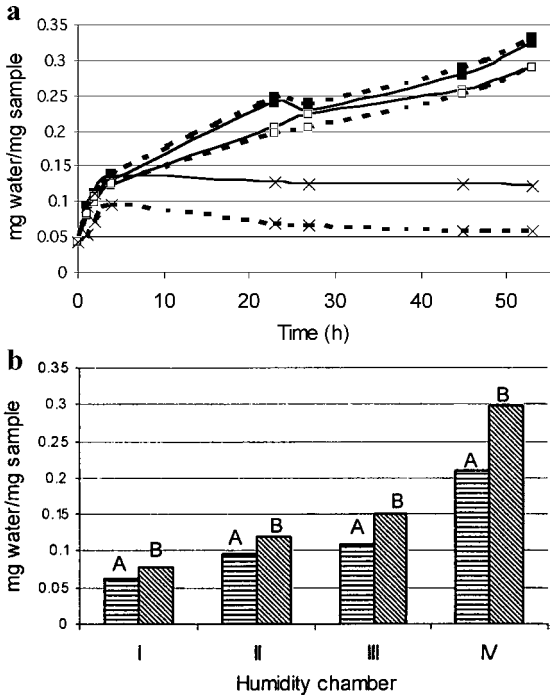

Figure 1. Water contents, calculated on a wet basis, for gluten samples in two hydration experiments. (**a**) Time series experiment. The samples were measured regularly during 53 h while kept in a humid chamber at 25 °C [G25A–D (■, ×)] or at 5 °C [G05A,B (□)]. The two samples G25C,D (×) were returned to a chamber with drying agent after 4 h of moistening. (**b**) Humidity chamber experiment. All samples were kept for 40 h above water (I, IV) or saturated solutions of $MgCl_2$ (II) or NaCl (III). One sample (I) was dried after initial moistening for 24 h above water. A, gluten prepared without salt; B, gluten prepared with salt in the wash water.

Spectral Pretreatment. The NIR reflectance spectra of gluten powders at different moisture contents are shown in **Figure 2a**. These spectra are greatly influenced by light scattering phenomena, which cause baseline shifting and likely result from changes in particle sizes and refractive index differences, as water is absorbed. With increasing water content, the increasing particle size and decreasing refractive index differences may cause decreasing scattering properties of the samples (higher baselines). To ease the spectral interpretation, several pretreatments were applied to get rid of these physical effects as well as the quantitative chemical variation that results from the different gluten/water ratios. One of the applied preprocessing methods was EMSC, which can be used for removing "physical" light scattering effects, including scaling effects as well as a polynomial baseline effect, without disturbing the chemical absorptions. In addition, the method is useful for correcting for unwanted "chemical" variations (*12*). This is done by including model spectra of the known interfering chemicals ("bad" spectra) as well as of the spectra of known chemical constituents ("good" spectra) in the EMSC model. In this physical−chemical EMSC, the contents of the bad components in each spectrum are estimated and their spectral contributions are modeled and subtracted according to eq 3. The spectral contributions of the good components are likewise modeled but not subtracted. Thus, EMSC was found to be beneficial for removing water contributions in the present case of NIR reflectance spectra, for which subtraction of the water spectrum is a complicated task.

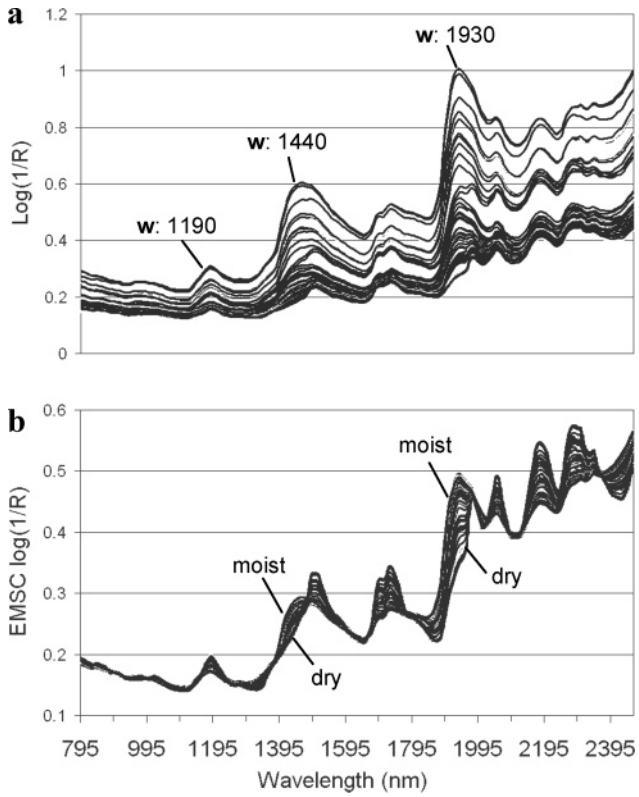

Figure 2. NIR reflectance spectra of dry and moistened gluten powder (0–33% mc): (**a**) raw spectra [the water bands (w) are marked]; (**b**) spectra corrected by physical EMSC.

The spectra resulting from a pure physical EMSC correction are shown in **Figure 2b**. Whereas some light scattering has been removed by this correction, the quantitative variation remains in these spectra. The major water peaks, found at 1190 nm (combination band, $2\cdot\nu_{1,3}+\nu_2$), 1440 (1, overtone band, $2\cdot\nu_{1,3}$), and 1930 nm (combination band, $\nu_{1,3}+\nu_2$), increase with increasing moisture content.

Subsequent second-derivative transformation reveals a quite complicated spectrum of gluten, in which several narrow protein peaks can be seen in some of the originally broad bands (**Figure 3a**). On the contrary, the second-derivative water spectrum (also indicated in **Figure 3a**) shows major features in the water band regions but only weak and broad bands in the remaining parts. Second-derivative transformation is not able to remove multiplicative/scaling effects, and these spectra contain large quantitative variations. Therefore, EMSC was applied again on the second-derivative data. The subsequent EMSC treatments included physical EMSC (**Figure 3b**) and a physical−chemical EMSC with a second-derivative water spectrum used as the "bad" spectrum (**Figure 3c**) as described under Materials and Methods. The latter procedure seemingly resulted in the best correction of the quantitative variations, and the spectra resulting from this pretreatment will be used in the further analyses. The regions below 1100 nm and above 2380 nm will be left out in the following analysis due to a high noise level in these regions.

PLS Regression. A PLS regression for prediction of the water contents (**y**), with the pretreated spectra (from **Figure 3c**) as **X**, was carried out. The resulting score plot of PC1 versus PC2 is shown in **Figure 4a**. The two PCs explain together 64.0% of the *X*-variance and 91.4% of the *Y*-variance. PC3 seemed to be related to the difference between the two gluten preparations (glutens A and B), but this PC was quite noisy, and adding more than two PCs to the model did not lead to any improvement in the prediction. The first two PCs seemed also somewhat influenced by noise, because very high-frequency features were apparent in the loading vectors, especially in the low-wavelength region. Removal of the nonsignificant variables found by jackknifing lead to a model with 92.5% explanation of the *Y*-variance and thus had only a small positive effect.

Score Plot Interpretation. The plot of PC1 scores versus the water content (**Figure 4b**) shows a monotonically increasing trend with a slope that seems to lessen after 10−15% mc. Likewise, for the course of the PC2 score, there is a breaking point at 12−15% mc. However, compared to PC1 scores, the PC2 scores show a different relationship to the moisture content: After an initial decrease, the scores increase again. These phenomena signify that the pretreated NIR spectra reflect some qualitative changes in the gluten system and not merely the different gluten/water ratios. Also, as both the time series and the hydration chamber experiments resulted in similar courses of the scores, it can be concluded that these spectral changes are not due to an effect of gluten aging (e.g., lipid oxidation) or to instrument drifts and day-to-day variations (e.g., due to changing temperature in the laboratory). Glutens A and B do not appear to be significantly distinct in the plots of PC1 and PC2 scores (**Figure 4a**), although moist gluten B samples show a little higher PC2 scores than gluten A samples at a given moisture content (not shown in **Figure 4**). Therefore, the salt treatment for gluten B does not seem to have influenced the two major spectral variations. Thus, it is again indicated that lipid oxidation or other lipid changes are not the main cause of the two spectral changes, because gluten A should otherwise be much more affected than gluten B (which contains less lipids).

It could be speculated that PC1, accounting for ∼55% of the spectral variance and ∼81% of the *Y*-variance, explains the binding of water to amino acids and the concurrent disruption of polymer−polymer interactions. These events are related to the lowering of T_g, and it is therefore interesting to note that Gontard et al. (*16*) observed a fast decrease of T_g until 10% mc, followed by a slower decrease of T_g with increasing mc in concordance with the here observed pattern of PC1 scores.

Figure 4c shows that PC2 scores for samples stored at 5 °C increase only little with increased mc (above 12−14%) as compared to samples stored at room temperature (25 °C). Therefore, PC2 could be related to glass transition changes, which take place for the 25 °C samples at 10−26% mc but first take onset at higher mc for the 5 °C samples (*13*). At the glass transition, the mobility of the gluten proteins is increased enough for aggregation to take place, and the porous structure is lost. This may explain the increased yellow/brown appearance of the 25 °C samples observed above a certain water content, although Maillard reactions may contribute as well to the color change (*15*). A proposal for the PC2 variation is that it reflects the progress from extensive protein−protein interactions in the dry state to the loosening of the structure upon water binding and then to formation of new polymer−polymer interactions, for example, in the intermolecular β-sheets.

Inspection of the scores for the samples that were slightly dried after an initial hydration period indicates that the hydration-induced changes are reversible. Two samples were moistened to 9.5 and 13.6% mc and thereafter dried in a drying chamber to 5.8 and 12.1% mc, respectively. These samples follow the same score pattern as the other samples, as shown in **Figure 4**. Their PC1 scores decrease after an initial increase and, thus, at least the PC1 variation seems to be reversible, implying that no major structural changes, for example, involving S−S interchanges, are taking place at these low water contents.

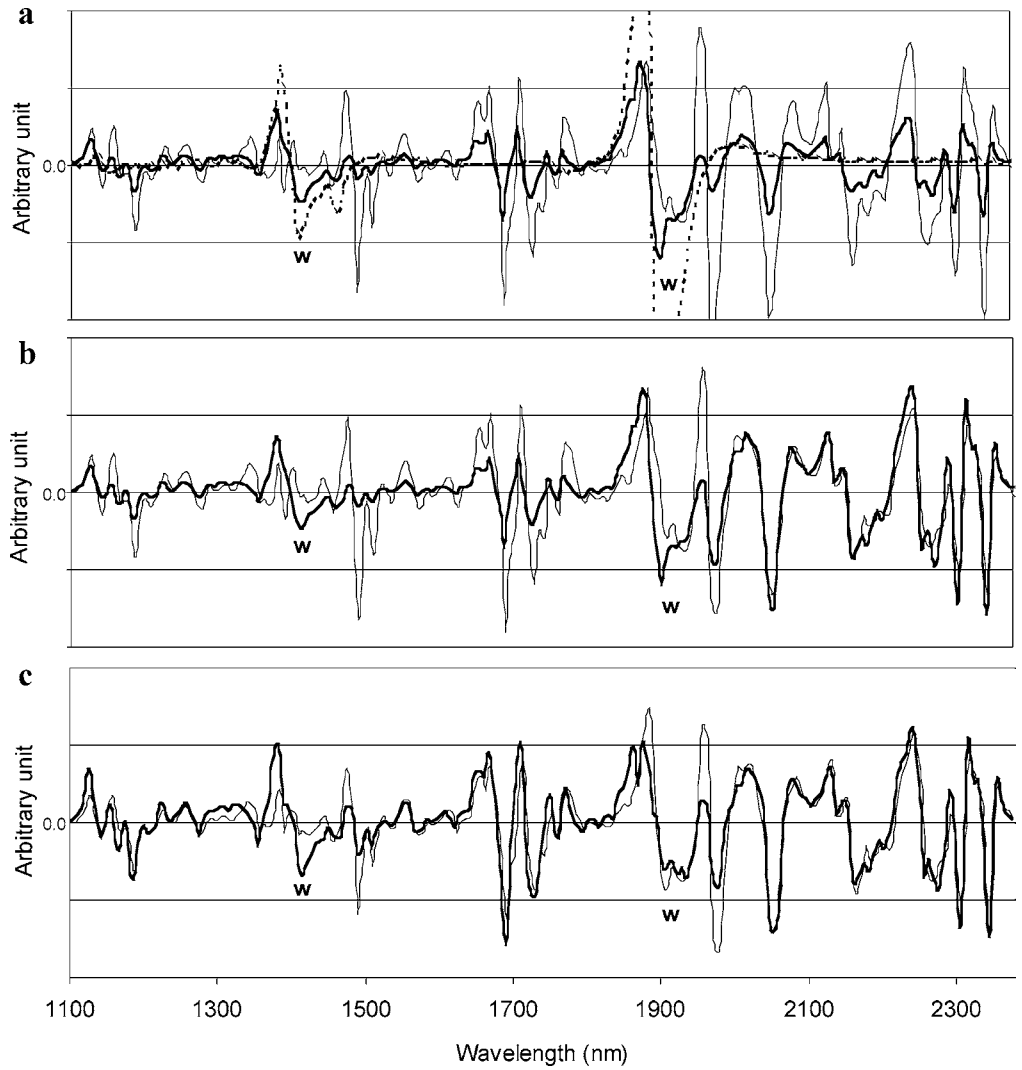

Figure 3. Second-derivative reflectance spectra (1100–2380 nm) of dry and moistened gluten powder (0–33% mc). The spectra of gluten at ~4% (—) and 33% mc (**—**) are shown as well as a water spectrum (- - -): (**a**) spectra corrected by physical EMSC and second-derivative transformation; **(b)** spectra in (**a**), additionally corrected by subsequent physical EMSC; (**c**) spectra in (**a**), additionally corrected by subsequent physical–chemical EMSC with removal of the second-derivative water spectrum, applied as "bad" spectrum in an EMSC.

However, reversibility in PC2 could not be confirmed, because samples in the short mc range had PC2 scores that were scattered more or less independently of the water content.

Spectral Interpretation. The PC1 and PC2 loading weight spectra ($\mathbf{p}_1$, $\mathbf{p}_2$) from the PLS regression were inspected for interpretation of the spectral changes described by the two PCs. Thus, the second-derivative spectra, representing a freeze-dried sample, a 12% mc, and a 33% mc sample, were calculated from the loadings and scores according to eq 4 as $\mathbf{x}_i = \mathbf{m} + t_{1,i}\cdot\mathbf{p}_1 + t_{2,i}\cdot\mathbf{p}_2$ for sample i, where the score values ($t_{1,i}$, $t_{2,i}$) are indicated in **Figure 4a**. The three artificial spectra (**Figure 5a**) show small differences, some of which are enlarged in **Figure 5b**,**c**. The spectral variations are interpreted with the caution that very high-frequency features may result from noise in the loading vectors. However, compared to the measured spectra, these calculated spectra are easier to interpret, because they contain less noise and do not contain irrelevant variations (e.g., the variation between gluten preparations).

This study has attention on two protein band regions, which are only little overlapped by the water bands, so as to avoid mistaken interpretations. The first region at 1610−1760 nm (**Figure 5b**) contains the first overtone of CH_x stretching vibrations mostly from amino acid side chains, whereas the second region at 2130−2320 nm (**Figure 5c**) contains combination bands of the amide vibrations (specific for proteins) as well as of the side-chain vibrations. The combination bands are, for example, seen at 2167 nm (amide B/II), 2184 nm (glutamine), 2209 nm (amide A/III), 2259 nm (OH str/OH def), 2280 nm (amide III/CH str or CH str/CH def), 2309 nm (CH str/CH def), and 2344 nm (CH str/CH def). The protein peaks and their proposed assignments according to refs *17*−*20* in the full combination band region are shown in **Table 1**. Jack-knifing showed most of the combination bands to be important in the prediction of the water content, with the exceptions of the amide A/II band at 2054 nm and the CH combination bands at 2309 and 2344 nm.

The spectral contributions from starch and lipid also need to be considered. Because it was previously indicated that lipid changes do not influence PC1 and PC2 much, only the influence of starch hydration was inspected. By comparison of the gluten and starch spectra (not shown) at increasing moisture content, it was found that starch hydration may contribute somewhat to the decreasing absorption at 1702 nm and the increasing absorption at 2282 nm in the spectra of increasingly moistened gluten. However, the effect may be small, as starch constitutes a minor fraction.

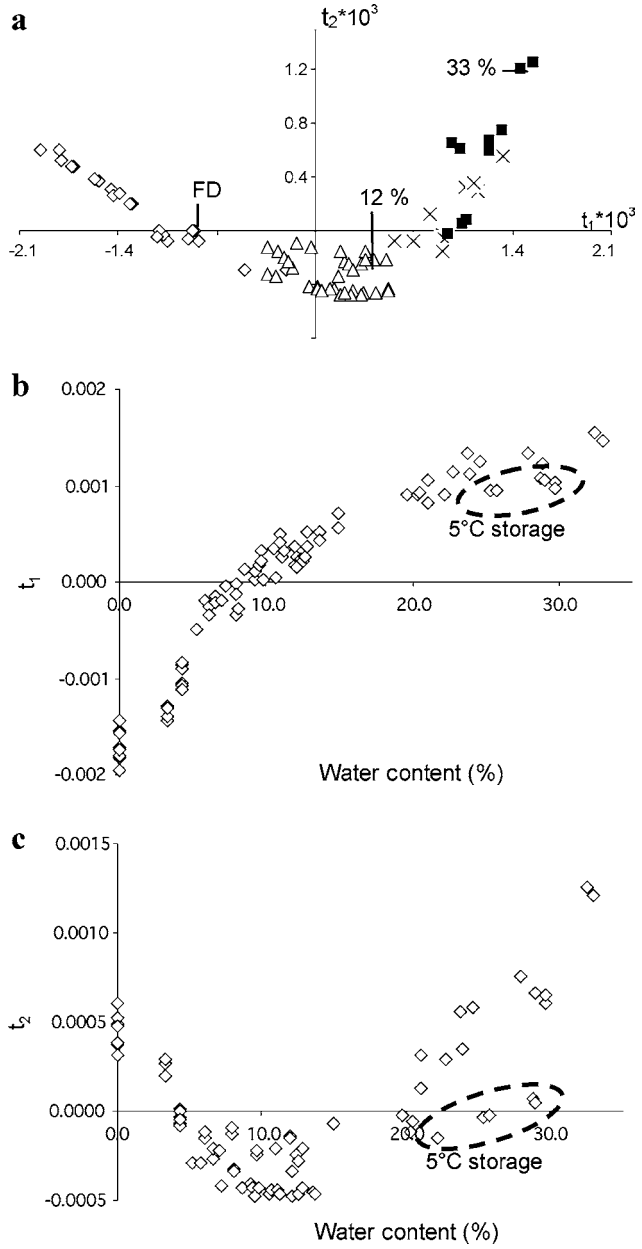

Figure 4. Score plots from a PLS regression. Gluten spectra (1100–2380 nm), pretreated as in **Figure 3c**, were used as **X** in a regression model for prediction of the moisture contents (*y*), ranging from ~0 to 33%. (**a**) PC1 scores vs PC2 scores for the samples of 0–6.0% mc (◇), 6.1–14.0% mc (△), 14.1–24.0% mc (×), and 24.1–33.0% (■). A freeze-dried sample (FD), a 12% mc, and a 33% mc sample are pointed out. (**b**) PC1 scores vs moisture content. (**c**) PC2 scores vs moisture content. Samples were hydrated until equilibrium at different relative humidities or for different time periods in a humid chamber. Samples stored at 5 °C during hydration are pointed out where they do not follow the trend of the samples stored at 25 °C. PC1 and PC2 explain 54.9 and 9.1% of the *X*-variance and 80.7 and 9.7% of the *Y*-variance, respectively.

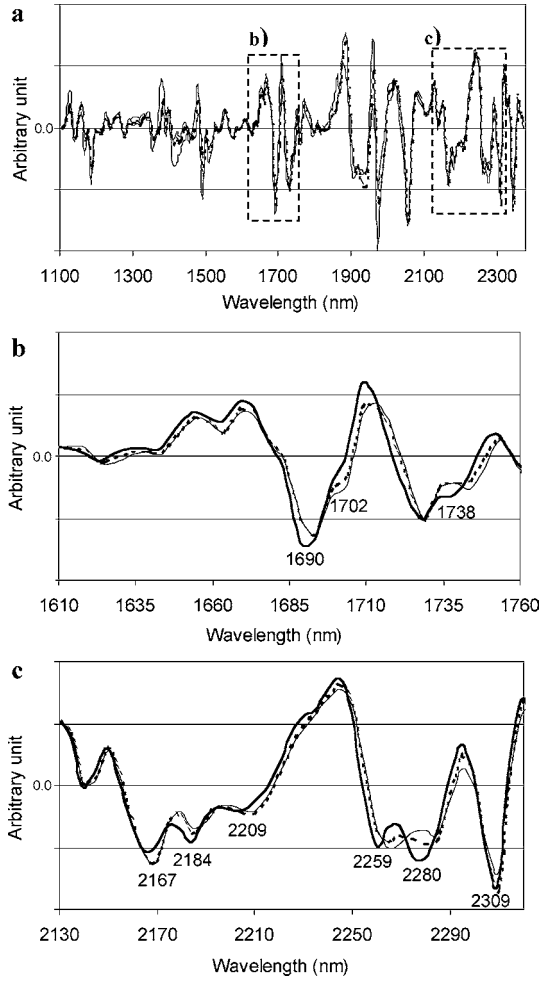

Figure 5. Calculated second-derivative NIR spectra, representing a freeze-dried (—), a 12% mc (- - -), and a 33% mc (**—**) gluten sample: (**a**) full wavelength region, 1100–2380 nm; (**b**) first overtones of CH_x-str, 1610–1760 nm; (**c**) amide and side-chain combination bands, 2130–2320 nm. The spectra were constructed from PC1 and PC2 loading weights and scores, obtained in a PLS regression for prediction of the moisture contents (*y*) from the preprocessed NIR spectra (*X*) (shown in **Figure 3c**).

Table 1. NIR Combination Bands and Their Assignments

wavelength (nm)	assignment
1975	glutamine (*17*)
2056	amide A/II (*18*)
2100–2120	amide B/I (*19*)
2141	
2167	amide B/II (*20*)
2184	glutamine (*21*)
2209	amide A/III (*19*)
2261	OH str/HOH def (*20*)
2281	amide III/CH_2 str (*20*)
2308	CH str/CH def
2346	CH str/CH def

Thus, the increasing intensity of the 1690 and 1738 nm peaks at the expense of the 1743 nm peak, which are the most prominent spectral changes in the C−H stretching overtone region (**Figure 5b**), can be attributed to changes in the gluten proteins upon moistening. These alterations, appearing as low-wavelength shifts of the two major peaks in this region, may be ascribed to changing microenvironments and interactions of the amino acid residues. Likewise, the increasing intensities at 2184, 2259, and 2276−2280 nm at the expense of the intensities of the 2167, 2209, and 2264 nm peaks (**Figure 5c**) can be explained from qualitative changes in the proteins. In one of the first studies of protein structures with NIR spectroscopy, Kamishikiryo-Yamashita et al. (*22*) considered the relative contributions from α-helix, *β*-sheet, and random coil to the intensity of the 2170 nm band and found that α-helices contribute the double of *β*-sheet and random coil to this band. According to the existing assignments of NIR wavelength regions to secondary structures by Robert et al. (*23*) (**Table 2**), the spectral changes in **Figure 5c** could be interpreted as an

Table 2. Assignments of NIR Regions to Secondary Structures[a]

structure	characteristic wavelengths (nm)
α-helix	2056, 2172,[b] 2239, 2289,[b] 2343
β-sheet (inter- and intra-)	2205, 2264, 2313
random	2265

[a] Taken from Robert et al. (*23*). [b] Most important wavelengths for α-helix.

increase of α-helix (2182 and 2280 nm) and a decrease of β-sheet (2209 and 2264 nm) and of random structure (2264 nm), of which only the latter change is in good agreement with previous gluten hydration studies. An ATR-FTIR study by Belton et al. (*14*) of the hydration-induced structure changes in glutenin and gliadin subunits has pointed to an initial decrease of random structure simultaneously with an increase of intra- and intermolecular β-sheet upon moistening of the dry proteins. Because both types of β-sheet absorb at ∼2209 nm, the decrease at this wavelength is obscure. Also, other phenomena imply that the spectral changes cannot be interpreted solely from **Table 2** and explained as secondary structure changes.

The contradictory behaviors of the 2167 nm peak (decreasing) and the 2182 nm peak (increasing), both found in a region commonly ascribed to α-helix, could be due to changing hydrogen-bonding strength of the NH oscillators existing in the α-helices. Murayama et al. (*20*) pointed out that the amide B/II frequency is sensitive to both secondary structure and the hydrogen-bonding strength in the structures. Thus, a shift to lower wavelengths of the amide B/II band has been taken as a sign of decreased hydrogen bonding, and in support of the above proposal, this has been observed upon loosening of the structures in molten globule formation (*20*). Shifts and splitting of the amide B/II band have also been reported frequently in other protein denaturation studies (*18*, *24*). In this regard, decreases of the 2170 nm peak and increases of the 2180 nm peak upon cooling and maturation of gelatin gels were explained by Segtnan et al. (*25*) from the conversion of single helices to triple helices with increased hydrogen bonding. In addition, the amide II mode is actually reported to be more sensitive to hydration per se than to the hydration-induced secondary structure changes (*26*).

Alternatively, the changes in amide B/II may be explained from the proposed contributions of glutamine and asparagine side-chains vibrations to the 2180−2190 nm band (*21*). Thus, the spectral changes may also reflect changing microenvironments and interaction states of these amino acid side chains. This hypothesis is supported by the large decrease of intensity in the 1975 nm peak, also ascribed to glutamine side chains (*17*). In addition, an ATR-FTIR study by Wellner et al. (*11*) has pointed to different hydrogen-bonding states of the glutamine side chains in dry and hydrated gluten. However, in the present study, the attribution of the apparent decrease in the 1975 nm band to changes in the glutamine side chains is ambiguous, because it as well may be an artifact, created in the preprocessing due to the close presence of the 1930 nm water band. Nevertheless, the proposal of perturbation of glutamine/asparagine side-chain absorptions is interesting in view of the participation of glutamine side chains in intermolecular β-sheet interactions and the proposal by Wellner et al. (*11*) of intra- and intermolecular hydrogen bonds between glutamine side chains and the protein backbone in the dry protein.

Other peaks from amino acid side chains show up in a region with a noticeable variation pattern. Several phenomena occur in the rather narrow region between 2250 and 2290 nm, as seen from the calculated spectra in **Figure 5c**. The details of these

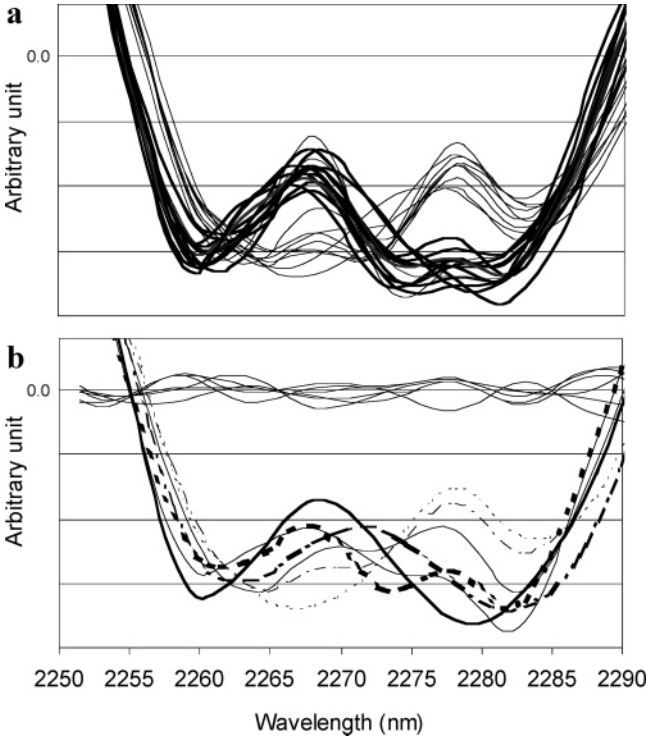

Figure 6. Second-derivative reflectance spectra with enlargement of a region (2250–2290 nm) with pronounced hydration-induced changes: (**a**) spectra of gluten samples at ∼0% mc (thin lines) and ∼25–33% mc (thick lines). (**b**) spectra of gluten samples at ∼0% mc (thin dotted line), 4% mc (thin dashed line), 7% mc (thin line), 12% mc (normal dashed line), 20% mc (normal line), 25% mc (thick dashed line), and 30% mc (thick line). The NIR spectra have been preprocessed as in **Figure 3c**. The residuals (lines close to zero) show the difference between these spectra and their corresponding spectra calculated from PC1 and PC2 loading weights and scores. These parameters were obtained in a PLS regression on the whole data set for prediction of the moisture contents (*y*) from the preprocessed NIR region 2250–2290 nm (*X*).

variations are seen more clearly in the enlargement in **Figure 6**, which presents some of the original pretreated spectra. The replicate variability in the 2250−2290 nm region is demonstrated in **Figure 6a** as several spectra of dry gluten are plotted, and the figure shows that the distinction between dry gluten and gluten at the highest hydration level is obvious and not disturbed by replicate variations. **Figure 6b** shows how the spectra gradually change from one extreme to the other at increasing moisture content. A general trend is evident despite some noise. To demonstrate how well these original spectra can be reconstructed from loadings and scores, the differences between the two sets of spectra are shown in **Figure 6b** as well.

Whereas the absorbance at 2259 nm somewhat increases, there is a large decrease at 2264 nm, and this is seen as a low-wavelength shift and a narrowing of the peak at ∼2262 nm [OH str/HOH def (*20*)]. Also at 2274−2283 nm, there is a large increase, which results in an apparent low-wavelength shift of the peak at ∼2280 nm [amide III/CH str (*20*) or CH str/CH def]. Likewise, Sefara et al. (*27*) observed complex changes in this wavelength region upon solvent denaturation of β-lactoglobulin and explained this by changes in the side-chain interactions, as α-helix was converted to β-sheet. The peak at 2259 nm, ascribed to an OH combination mode (*20*), could likely reflect the interaction states of serine and tyrosine residues, which are found in the repetitive domains of gluten proteins. However, it should be stressed that a peak in NIR spectra cannot be ascribed to a single amino acid.

Table 3. Summary of Hydration- and Denaturation-Induced Spectral Effects

treatment	spectral effects	interpretation
hydration	2167↓ 2182↑	α-helix?
	2209↓ 2264↓	β-sheet and random structure↓
	1975↓ 2182↑	Gln and Asn side chains
	2259↑	Pro side chains
	2280↑	α-helix↑ side chains
	1690↑ 1700↓ 1738↑ 1743↓	
denaturation	2167↓ 2182↓	α-helix↓
	2209↑	β-sheet↑
	1975↓ 2182↓	Gln and Asn side chains
	2044↓	weakly hydrogen-bonded structure↓
	2280↓	α-helix↓
	1690↑ 1728↑ 1738↓ 1743↓ 1762↑	

Also, Segtnan et al. (*25*) observed increases at both 2256 and 2282 nm when gelatin gels were heated above their melting temperature. Because melting causes the basic unit in collagen, the polyproline II helix, to unfold from triple to single helixes, changes in proline side-chain microenvironments could likely be the cause of some of the spectral effects in the CH combination bands. This hypothesis is supported by an ATR-FTIR study, in which hydration of the dry poly(L-proline) protein caused high-wavelength shifts of the CH deformation bands, explained by an exchange of protein−protein interactions with protein−water interactions (*11*). Particularly, the above findings are relevant for gluten proteins as they contain high amounts of proline.

The speculation that CH bands are affected by structural alterations other than secondary structure changes is supported in a study of ovalbumin by Murayama et al. (*20*), in which changes in the CH combination bands (2342 nm) were observed, despite only minor secondary structure changes taking place upon lowering of the pH. The changes were thus ascribed to changing microenvironments of aromatic amino acid residues in a small conformation change (*20*).

In conclusion, from the hydration experiment, the spectral effects of gluten hydration, summarized in **Table 3**, may be interpreted mostly as direct effects of water binding to the gluten proteins. The indication of only small secondary structure changes is in agreement with other gluten hydration studies reporting large secondary structure changes only at water contents above 38% (*11*).

Gluten Denaturation. NIR spectra of moist (20−25% mc) and dry gluten before and after heat treatments at 65 or 85 °C were pretreated similarly to the samples in the hydration experiment, before the 1100−2380 nm region was submitted to a PCA. PC1 from this analysis explains 57% of the spectral variance and is related to the previously described effect of the water content on gluten, as judged by comparison to the hydration experiment and by interpreting the score plot for PC1 (not shown). This PC describes only the drying of the samples taking place during the heat treatment.

The score plot of PC2 versus PC3 (**Figure 7**) reveals that the samples treated by moisture and heat (65 or 85 °C) can be distinguished from the native gluten samples (dry and moist), as they form a separate group in the plot. However, the different heating times (0.5−1.5 h) do not appear to influence the PC2 and PC3 scores. Georget et al. (*28*) observed structural changes above 45 °C for 13% moist gluten, so the indicated denaturation at 65 °C is not unlikely. The indication that PC2 and PC3 are related to protein denaturation is further supported by the fact that the dry but heat-treated samples, which are not expected

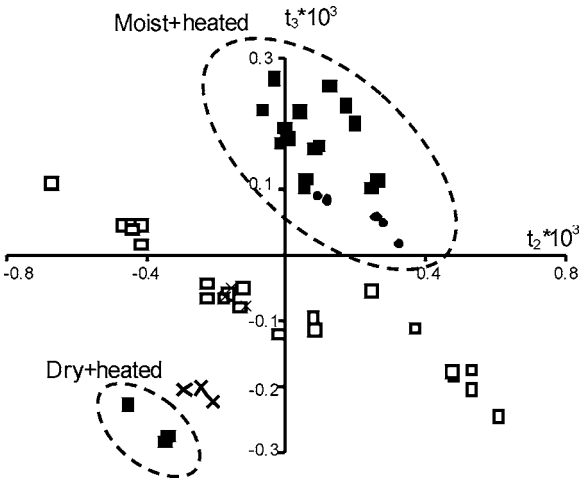

Figure 7. PCA score plot (PC2 scores vs PC3 scores) resulting from analysis of NIR spectra of native and heat-treated gluten. The spectra (1100–2380 nm) were pretreated as in **Figure 3c**. Gluten powder samples were moistened to 20–25% mc. Moist (□) and dry (×) samples were submitted to heating in a water bath at 65 °C (●) or 85 °C (■). A moist sample was dried instead (□). PC2 and PC3 explain 12 and 3%, respectively, of the spectral variance.

to be denatured (*28*), are placed close to the dry native samples in the score plot. However, the score plot reveals a lot of replicate variability in the two PCs. Also, the observed effects of the denaturation are small, and PC2 and PC3 explain only ∼12 and 3%, respectively, of the total variance. This is not unexpected, because structural reversion during cooling of heat-treated gluten has been shown to leave only small permanent structure changes in gluten at low water contents (*28*).

To determine the significant NIR variables, a discriminant PLS regression was carried out ($\mathbf{X}$ = NIR spectra, $\mathbf{y}$ = indicator variable: denatured/native) with jack-knifing. The model used four PCs and resulted in a correlation of 0.95. Only the hereby-determined significant NIR wavelengths will be considered in the following.

Spectral Interpretation. Spectra, representing a native, a denatured, and an extensively denatured sample, were calculated from PCA scores and loadings according to eq 4 as $\mathbf{x}_i = \mathbf{m} + t_{3,i}\cdot\mathbf{p}_3$ for sample i. The score values ($t_{3,i}$) were -0.1×10^{-3}, 0.2×10^{-3}, and 0.4×10^{-3} for the three spectra, respectively. (PC2 was not included in the calculation because it represents mostly replicate variability.) The calculated spectra are shown in **Figure 8** for the combination band region (1940−2220 nm), showing the largest variations, which, however, are small compared to the hydration-induced changes. Changes were also seen at 1610−1760 nm (first overtone region), but they were quite small, and they are shown only in **Table 3**, summarizing all of the spectral changes in the two regions and their interpretation.

In the combination band region, the most prominent change is an increase at 2209 nm and decreases at 2167 and 2182 nm (**Figure 8**), which may stem from an increase of β-sheet at the expense of α-helix upon denaturation (see **Table 2**) in agreement with ATR-FTIR studies of gluten denaturation (*28*, *29*). Georget et al. (*28*) have suggested that α-helices may unfold and form intermolecular β-sheet upon the heat denaturation and that the changes are made irreversible by the formation of sulfur bridges. However, their results showed that the structural changes and their permanence highly depended on the water content (*28*). The decrease at 2182 nm could, as discussed previously, also be due to decreased water interaction of glutamine side chains.

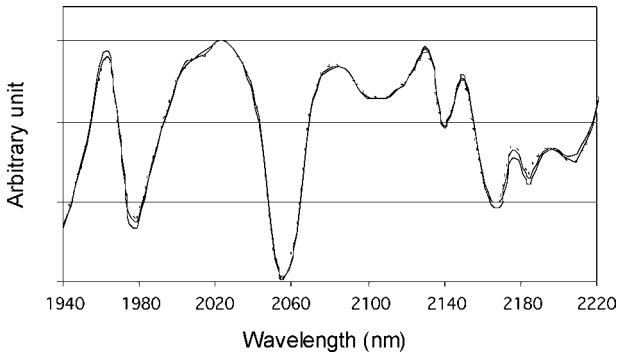

Figure 8. Calculated second-derivative NIR spectra, representing a moist native (normal line), a moderately denatured (thin line), and a highly denatured (thin dashed line) gluten sample. The spectra were constructed from PC3 loadings and scores, which were obtained in a PCA of the pretreated spectra.

Here, both of the peaks ascribed to glutamine and asparagine side chains at 1975 and 2182 nm show decreases upon denaturation, whereas they showed a decrease and an increase, respectively, upon hydration. This controversy suggests that the 1975 nm peak is affected by the overlapping water band and is unreliable.

Although the region 2250−2290 nm is suggested to be sensitive to the secondary structures, no significant changes are seen in this region upon gluten denaturation, except for a minor decrease at 2289 nm (not shown), again indicating a decrease of α-helix, although an increase of random structure (2264 nm) could have been expected according to results of Mangavel et al. (*29*).

In the amide combination band region, a hardly discernible decrease on the low-wavelength side of the amide A/II band (2054 nm) is seen (**Figure 8**). This band has been demonstrated to be sensitive to protein denaturation, even though its ability to discriminate between secondary structures is vague (*18*, *30*). In studies of the heat denaturation of ovalbumin and human serum albumin, shifts to lower wavelengths of this band were seen upon unfolding of the secondary structure (*18*, *30*). For gluten, the opposite shift could indicate a strengthening of the structure due to intermolecular β-sheet formation.

Final Remarks. NIR spectroscopy has become widely applied as a method for quality control in the agricultural, pharmaceutical, and food industries, etc. However, the method has seldom been applied for protein structure analysis, and the relationship between NIR spectra and protein secondary structures was not recognized until the early 1990s (*22*). The correspondence between protein secondary structure and band shape and position in the combination band region has since been established in studies of freeze-dried proteins (*23*). As a consequence, NIR spectroscopy could also be expected to provide useful information on the gluten protein structures and interactions, which are of utmost importance to the functionality of gluten powders. The obvious advantages of NIR over FTIR spectroscopy are the higher speed of measurements and the deeper penetration of the NIR light. A disadvantage is the difficulty of interpreting the NIR spectra, due to lack of peak assignments and limited research on the relationship between NIR absorptions and protein secondary structures.

Although the variations in the gluten NIR spectrum were not fully explicable, this study has shown that NIR spectroscopy may be able to give important information on hydration and structure changes in the gluten proteins, as here demonstrated for a system with high protein content and low content of other components such as starch and water.

Certainly, a more comprehensive interpretation of the gluten NIR spectrum will require the use of both ATR-FTIR (to obtain the secondary structures) and NMR (to obtain the side-chain interactions) as reference methods. NMR may be the most important, because the present NIR study indicated that the water−side-chain interactions cause spectral effects that are dominant compared to the secondary structure effects. In this respect, NIR spectroscopy could be better suited than FTIR spectroscopy for detecting the interaction state of glutamine side chains, because these side-chain absorptions are highly overlapped by the amide bands in MIR. The involvement of glutamine side chains in hydrogen bond interactions with the protein backbone in dry gluten and in intermolecular β-sheet interactions in hydrated gluten has been indicated from FTIR and solid-state NMR studies, respectively (*11*, *31*). Thus, studies of the glutamine side-chain interactions are highly relevant due to the suggested importance of the intermolecular β-sheet to the viscoelastic properties of gluten.

ABBREVIATIONS USED

ATR, attenuated total reflectance; EMSC, extended multiplicative scatter correction; FTIR, Fourier transform infrared; mc, moisture content; MIR, midinfrared; NIR, near-infrared; PCA, principal component analysis; PC, principal component; PLS, partial least squares; RH, relative humidity.

ACKNOWLEDGMENT

Harald Martens (Norwegian Food Research Institute) is greatly thanked for his support on EMSC.

LITERATURE CITED

(1) Tolstoguzov, V. Structure−property relationships in foods. In *Macromolecular Interactions in Food Technology*; Parris, N., Kato, A., Creamer, L. K., Pearce, J., Eds.; American Chemical Society: Washington, DC, 1996; pp 2−14.

(2) Ibanez, E.; Cifuentes, A. New analytical techniques in food science. *Crit. Rev. Food Sci. Nutr.* **2001**, *41*, 413−450.

(3) Haris, P. I.; Severcan, F. FTIR spectroscopic characterization of protein structure in aqueous and non-aqueous media. *J. Mol. Catal. B: Enzym.* **1999**, *7*, 207−221.

(4) Barth, A.; Zscherp, C. What vibrations tell us about proteins. *Q. Rev. Biophys.* **2002**, *35*, 369−430.

(5) Pezolet, M.; Bonenfant, S.; Dousseau, F.; Popineau, Y. Functional and solution states as determined by infrared-spectroscopy. *FEBS Lett.* **1992**, *299*, 247−250.

(6) Belton, P. S. On the elasticity of wheat gluten. *J. Cereal Sci.* **1999**, *29*, 103−107.

(7) Lindsay, M. P.; Skerrit, J. H. The glutenin macropolymer of wheat flour doughs: structure−function perspectives. *Trends Food Sci. Technol.* **1999**, *10*, 247−253.

(8) Veraverbeke, W. S.; Delcour, J. A. Wheat protein composition and properties of wheat glutenin in relation to breadmaking functionality. *Crit. Rev. Food Sci.* **2002**, *42*, 179−208.

(9) Pezolet, M.; Bonenfant, S.; Dousseau, F.; Popineau, Y. Conformation of wheat gluten proteins. Comparison between functional and solution states as determined by infrared-spectroscopy. *FEBS Lett.* **1992**, *299*, 247−250.

(10) Wellner, N.; Mills, E. N. C.; Browsney, G.; Wilson, R. H.; Brown, N.; Freeman, J.; Halford, N. G.; Shewry, P. R.; Belton, P. S. Changes in protein secondary structure during gluten deformation studied by dynamic Fourier transform infrared spectroscopy. *Biomacromolecules* **2005**, *6*, 255−261.

(11) Wellner, N.; Belton, P. S.; Tatham, A. S. Fourier transform IR spectroscopic study of hydration-induced structure changes in the solid state of ω-gliadins. *Biochem. J.* **1996**, *319*, 741−747.

(12) Martens, H.; Nielsen, J. P.; Engelsen, S. B. Light scattering and light absorbance separated by extended multiplicative signal correction. Application to near-infrared transmission analysis of powder mixtures. *Anal. Chem*. **2003**, *75*, 394−404.
(13) Cherian, G.; Chinachot, P. ^{2}H and ^{17}O Nuclear magnetic resonance study of water in gluten in the glassy and rubbery state. *Cereal Chem.* **1996**, *73*, 618−624.
(14) Belton, P. S.; Colquhoun, I. J.; Grant, A.; Wellner, N.; Field, J. M.; Shewry, P. R.; Tatham, A. S. FTIR and NMR-studies on the hydration of high-M(R) subunit of glutenin. *Int. J. Biol*. **1995**, *17*, 74−80.
(15) Elizalde, B. E.; Pilosof, A. M. R. Kinetics of physico-chemical changes in wheat gluten in the vicinity of the glass transition temperature. *J. Food Eng*. **1999**, *42*, 97−102.
(16) Gontard, N.; Ring, S. Edible wheat gluten film: influence of water content on glass transition temperature. *J. Agric. Food Chem*. **1996**, *44*, 3474−3478.
(17) Holly, S.; Egyed, O.; Jalsovszky, G. Assignment problems of amino acids. Dipeptides and tripeptides and proteins in the near-infrared region. *Spectrochim. Acta A* **1992**, *48*, 101−109.
(18) Wang, Y.; Murayama, K.; Myojo, Y.; Tsenkova, R.; Hayashi, N.; Ozaki, Y. Two-dimensional Fourier transform near-infrared spectroscopy study of heat denaturation of ovalbumin in aqueous solutions. *J. Phys. Chem. B* **1998**, *102*, 6655−6662.
(19) Czarnik-Matusewicz, B.; Murayama, K.; Tsenkova, R.; Ozaki, Y. Analysis of near-infrared spectra of complicated biological fluids by two-dimensional correlation spectroscopy: protein and fat concentration-dependent spectral changes of milk. *Appl. Spectrosc*. **1999**, *53*, 1582−1594.
(20) Murayama, K.; Ozaki, Y. Two-dimensional near-IR correlation spectroscopy study of molten globule-like state of ovalbumin in acidic pH region: simultaneous changes in hydration and secondary structure. *Biopolymers* **2002**, *67*, 394−405.
(21) Yamashita, H.; Takamura, H.; Matoba, T. Effect of non-peptide and non-protein nitrogen compounds for the determination of protein content by near infrared spectroscopy. *J. Near Infrared Spec*. **1994**, *2*, 145−151.
(22) Kamishikiryo-Yamashita, H.; Tatara, M.; Takamura, H.; Matoba, T. Effect of secondary structures of protein on determination of protein-content by near-infrared spectroscopy. *J. Jpn. Soc. Food Sci. Technol*. **1994**, *41*, 65−69.
(23) Robert, P.; Devaux, M. F.; Mouhous, N.; Dufour, E. Monitoring the secondary structure of proteins by near-infrared spectroscopy. *Appl. Spectrosc*. **1999**, *53*, 226−232.
(24) Yuan, B.; Muayama, K.; Wu, Y. Q.; Tsenkova, R.; Dou, X. M.; Era, S.; Ozaki, Y. Temperature-dependent near-infrared spectra of bovine serum albumin in aqueous solutions: spectral analysis by principal component analysis and evolving factor analysis. *Appl. Spectrosc*. **2003**, *57*, 1223−1229.
(25) Segtnan, V. H.; Isaksson, T. Temperature, sample and time dependent structural characteristics of gelatine gels studied by near infrared spectroscopy. *Food Hydrocolloids* **2004**, *18*, 1−11.
(26) Pevsner, A.; Diem, M. Infrared spectroscopic studies of major cellular components. Part I: the effect of hydration on the spectra of proteins. *Appl. Spectrosc.* **2001**, *55*, 788−793.
(27) Sefara, N. L.; Magtoto, N. P.; Richardson, H. H. Structural characterization of β-lactoglobulin in solution using two-dimensional FT mid-infrared and FT near-infrared correlation spectroscopy. *Appl. Spectrosc.* **1997**, *51*, 536−540.
(28) Georget, D. M. R.; Belton, P. S. Effects of temperature and water content on the secondary structure of wheat gluten studied by FTIR spectroscopy. *Biomacromolecules* **2006**, *7*, 469−475.
(29) Mangavel, C.; Barbot, J.; Popineau, Y.; Gueguen, J. Evolution of wheat gliadins conformation during film formation: a Fourier transform infrared study. *J. Agric. Food Chem*. **2001**, *49*, 867−872.
(30) Wu, Y. Q.; Czarnik-Matusewicz, B.; Murayama, K.; Ozaki, Y. Two-dimensional near-infrared spectroscopy study of human serum albumin in aqueous solutions: using overtones and combination modes to monitor temperature-dependent changes in the secondary structure. *J. Phys. Chem. B* **2000**, *104*, 5840−5847.
(31) Alberti, E.; Humpfer, E.; Spraul, M.; Gilbert, S. M.; Tatham, A. S.; Shewry, P. R.; Gil, A. M. A high resolution ^{1}H magic angle spinning NMR study of a high-M_r subunit of wheat glutenin. *Biopolymers* **2000**, *85*, 33−45.

Received for review December 19, 2006. Revised manuscript received May 30, 2007. Accepted June 14, 2007. The Technical University of Denmark is thanked for a 3 year grant to S.W.B.

JF063680J